radius at the waist position z_0, we fit the measured beam radius and obtain the M^2 factor. As shown in Figure 7, the best-fit value of M^2 is 1.24 $\pm$ 0.03 (two standard deviations) with 20 W of output average power, which confirms the diffraction-limited beam quality and SM operation of the coiled amplifier. No appreciable change in M^2 was observed as a function of pump power.

4. CONCLUSIONS

In this article, we have demonstrated an all-fiber MOPA system that has produced as much as 20-W average power of output with nanosecond pulse and near diffraction-limited beam quality (M^2 = 1.24 $\pm$ 0.03). The repetition rate can be changed during 50–175 kHz while the pulse duration can be fixed at 15 ns. Based on this system, the impacts of seed power on amplification capability are systematically investigated. We found that the signal cannot be amplified unlimitedly at one certain pump power; there exists a maximum of seed power which is sufficient to saturate this all-fiber amplifier. By increasing the repetition rate, further power scaling can be provided. Saturation was not observed during the whole amplification; therefore, we believed that the maximum average power of output in our system was limited by the available pump power.

The all-fiber MOPA system employs a simple and compact architecture and is therefore suitable for the use in practical applications. Because of the high energy, high repetition rate, and diffraction-limited beam quality, this laser can be used in materials processing, remote sensing, and chemical detection.

REFERENCES

1. J. Limpert, S. Hofer, A. Liem, et al., 100-W average-power, high-energy nanosecond fiber amplifier, Appl Phys B 75 (2002), 477–479.
2. M.-Y. Cheng, Y.-C. Chang, A. Galvanauskas, et al., High-energy and high-peak-power nanosecond pulsegeneration with beam quality control in 200-mm core highly multimode Yb-doped fiber amplifiers, Opt Lett 30 (2005), 358–360.
3. L. Kong, Q. Lou, J. Zhou, et al., 133-W pulsed fiber amplifier with large mode area fiber, Opt Eng Lett 45 (2006), 010502.
4. M.W. Sasnet and T.F. Johnson, Proc SPIE 1414 (1991), 21.
5. H.M. Pask, R.J. Carman, D.C. Hanna, A.C. Tropper, C.J. Mackechnie, P.R. Barber, and J.M. Dawes, Ytterbium-doped silica fiber lasers: Versatile sources for the 1–1.2 μ m region, IEEE J Selected Top Quantum Electron 1 (1995), 2–13.
6. J.P. Koplow, D.A.V. Kliner, and L. Goldberg, Single-mode operation of a coiled multimode fiber amplifier, Opt Lett 25 (2000), 442.

HALF-WAVELENGTH LOOP STRIP CAPACITIVELY FED BY A PRINTED MONOPOLE FOR PENTA-BAND MOBILE PHONE ANTENNA

Yun-Wen Chi and Kin-Lu Wong
Department of Electrical Engineering, National Sun Yat-Sen University, Kaohsiung 80424, Taiwan; Corresponding author: wongkl@ema.ee.nsysu.edu.tw

Received 21 February 2008

ABSTRACT: *In this study, a novel internal penta-band antenna formed by a half-wavelength loop strip capacitively fed by a printed monopole for mobile phone application is proposed. The antenna is configured such that, inside the antenna region, possible electronic elements, such as the speaker or the like, can be embedded to achieve a compact integration of the antenna inside the mobile phone; moreover, the antenna performances can be very slightly affected by the integrated element. The antenna can further generate two wide resonant modes at about 900 and 1900 MHz for GSM850/900 and DCS/PCS/UMTS operation, respectively. In addition, the two resonant modes can generally be controlled separately, with the lower one controlled by the loop strip operated as a 0.5-wavelength structure and the upper one controlled by the printed monopole operated as a 0.25-wavelength structure. Detailed design considerations of the proposed antenna are presented.* © 2008 Wiley Periodicals, Inc. Microwave Opt Technol Lett 50: 2549–2554, 2008; Published online in Wiley InterScience (www.interscience.wiley.com). DOI 10.1002/mop.23769

Key words: *mobile phone antennas; loop antennas; printed monopoles; penta-band operation; internal mobile phone antennas*

1. INTRODUCTION

Recently, the loop antennas have been shown to be very promising for application in the mobile phone as internal multiband antennas for wireless wide area network (WWAN) communications [1–5]. These multiband loop antennas cover several or all operating bands in the GSM850 (824–894 MHz), GSM900 (890–960 MHz), DCS (1710–1880 MHz), PCS (1850–1990 MHz), and UMTS (1920–2170 MHz) systems [6]. With multiband operation obtained, these loop antennas occupy reasonable volume inside the mobile phone. However, these antennas are mainly designed to stand alone inside the mobile phone and cannot be integrated with the nearby electronic elements such as the speaker [7, 8] or the like.

In this study, we demonstrate a novel internal penta-band loop antenna promising for integration with the speaker in the mobile phone. The antenna is mainly formed by a half-wavelength loop strip capacitively fed by a printed monopole. The loop strip is of a narrow width (1 mm here) and is configured to have a compact configuration at the top no-ground region of the system circuit board of the mobile phone. Different from the monopole antenna where the wider monopole can lead to a wider operating bandwidth [9–11], the achievable bandwidth of the loop antenna is generally very slightly affected by reducing its width. This feature is an advantage for the loop antenna, especially for its possible application in the mobile phone for GSM operation. Hence, although a long half-wavelength strip is required for resonating at about 900 MHz, we can use a narrow strip to form the loop antenna to generate the required bandwidth to cover the GSM850/900 band. This makes the loop antenna in this study have a small occupied area and a simple structure as well, which makes it easy to fabricate for practical applications.

To excite the loop strip, a simple monopole strip printed on the top no-ground region of the system circuit board is used. Through capacitive coupling [12, 13], the loop strip can resonate at about 900 MHz to generate a half-wavelength loop mode for GSM850/900 operation. Moreover, the printed monopole alone can resonate at about 1900 MHz to generate a wide operating band to cover DCS/PCS/UMTS operation. The proposed antenna can hence generate two wide operating bands at about 900 and 1900 MHz, which can generally be controlled separately by the loop strip and the printed monopole, respectively, for covering GSM850/900 and DCS/PCS/UMTS operation. Detailed design considerations of the proposed internal penta-band antenna for mobile phone applications are described. Results of the constructed prototype are presented and discussed. In addition, the case of the proposed antenna embedded with a practical speaker is studied.

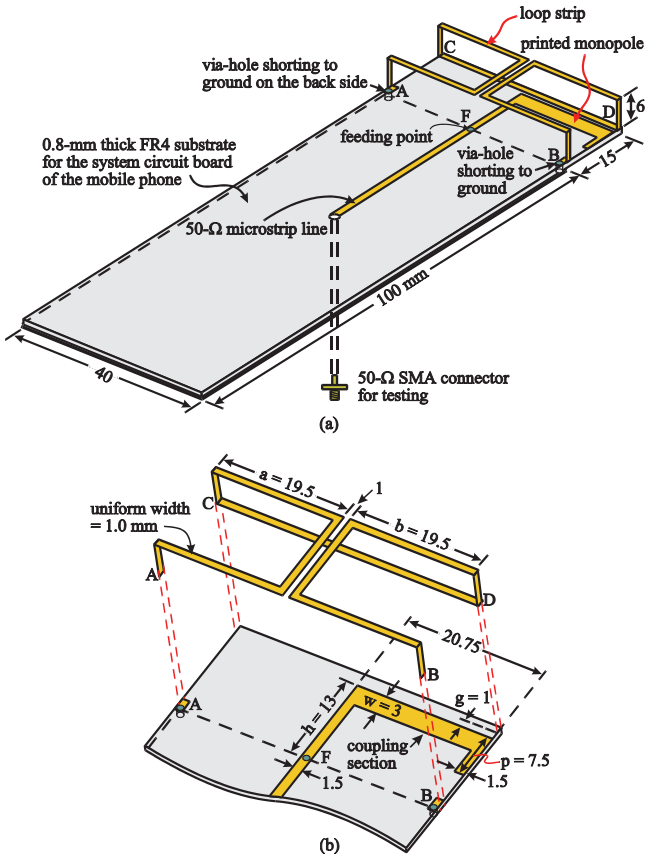

Figure 1 (a) Geometry of the proposed antenna in the mobile phone. (b) Detailed dimensions of the antenna. [Color figure can be viewed in the online issue, which is available at www.interscience.wiley.com]

2. DESIGN CONSIDERATIONS OF PROPOSED ANTENNA

Figure 1 shows the configuration of the proposed antenna formed by a loop strip and a printed monopole. As shown in Figure 1(a), the antenna occupies a volume of $6 \times 15 \times 40$ mm^3 or 3.6 cm^3 and is placed on the top no-ground region of the 0.8-mm thick FR4 substrate (system circuit board of the mobile phone). On the back side of the circuit board, there is a printed ground plane of size 40×100 mm^2, leaving a top no-ground region of size 40×15 mm^2 on the circuit board. The loop strip has a uniform width of 1 mm and a length of 170 mm, starting from point A, through points C and D, to point B. Note that the section $\overline{CD}$ is printed on the top edge of the no-ground region in this study for easy fabrication, whereas the remaining loop strip above the circuit board is cut from a copper plate and then folded into the compact configuration as shown in the figure. By further including the top edge ($\overline{AB}$) of the ground plane, the loop strip forms a closed path of length 210 mm (about 0.63 λ at 900 MHz), allowing it to resonate as a half-wavelength loop structure at about 900 MHz for GSM850/900 operation. Detailed dimensions of the loop strip are given in Figure 1(b).

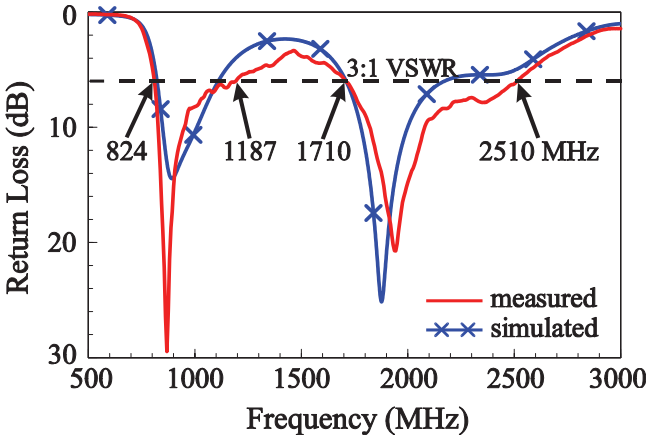

Figure 2 Measured and simulated return loss for the proposed antenna. [Color figure can be viewed in the online issue, which is available at www.interscience.wiley.com]

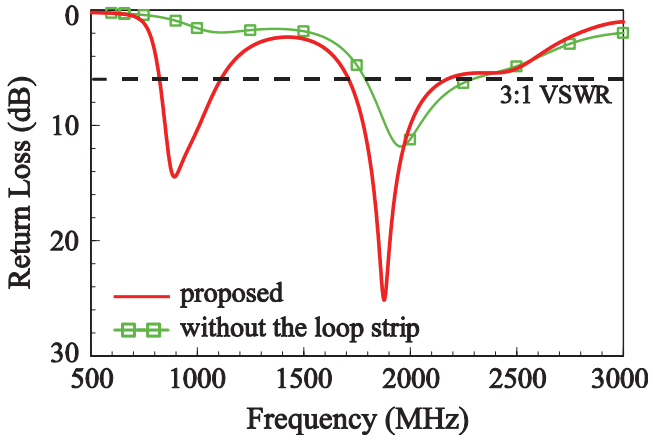

Figure 3 Comparison of the simulated return loss for the proposed antenna and the case without the loop strip. [Color figure can be viewed in the online issue, which is available at www.interscience.wiley.com]

In this study, the loop strip is capacitively excited by the printed monopole through a coupling gap of width (g) 1 mm. The printed monopole comprises a front section of length (h) 13 mm along the central line of the circuit board, a coupling section of width (w) 3 mm and length 20.75 mm, and an end section of length (p) 7.5 mm and width 1.5 mm. The total mean length of the printed monopole starting from point F (the feeding point of the antenna) to the open end is about 36 mm (about 0.23 λ at 1900 MHz), which makes it promising to generate a quarter-wavelength resonant mode at about 1900 MHz. By selecting a wide width of 3 mm (w) in the coupling section of the printed monopole, an operating band wide enough to cover DCS/PCS/UMTS operation is obtained. Also, note that the width of the front section of the printed monopole is selected to be 1.5 mm, the same as that of the 50-Ω microstrip feedline printed on the front side of the circuit board, to avoid discontinuity in the line width at the antenna's feeding point (point F). More detailed effects of the parameters g, w, and p will be discussed with the aid of Figures 5 and 6 in Section 3.

Also, note that the printed monopole occupies only a small portion of the top no-ground region, leaving a large portion of it suitable for accommodating the nearby electronic element such as the speaker in the mobile phone. In this study, the case of embedding a practical speaker inside the antenna region is studied in Figure 7 in the next section.

3. RESULTS AND DISCUSSION

Based on the design dimensions shown in Figure 1, which are the preferred dimensions in this study, the proposed antenna was constructed and tested. Figure 2 shows the measured and simulated return loss of the constructed prototype. The simulated results are obtained using Ansoft HFSS [14], and good agreement between the measurement and simulation is seen. As expected, two reso-

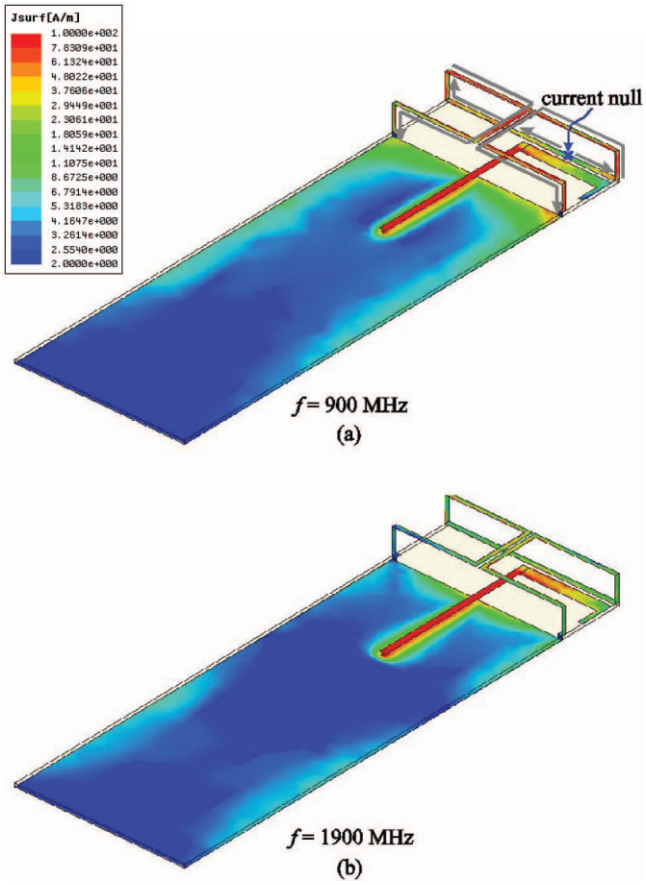

Figure 4 Simulated excited surface currents at 900 and 1900 MHz on the antenna and the system ground plane. [Color figure can be viewed in the online issue, which is available at www.interscience.wiley.com]

nant modes with good impedance matching are excited. The lower mode is at about 900 MHz with a large bandwidth of 363 MHz (824–1187 MHz), suitable for GSM850/900 operation. For the upper mode, it is at about 1900 MHz with a large bandwidth of 800 MHz (1710–2510 MHz) and is suitable for DCS/PCS/UMTS operation. Note that the bandwidth definition used here is 3:1 VSWR, which is a general standard for practical mobile phone applications.

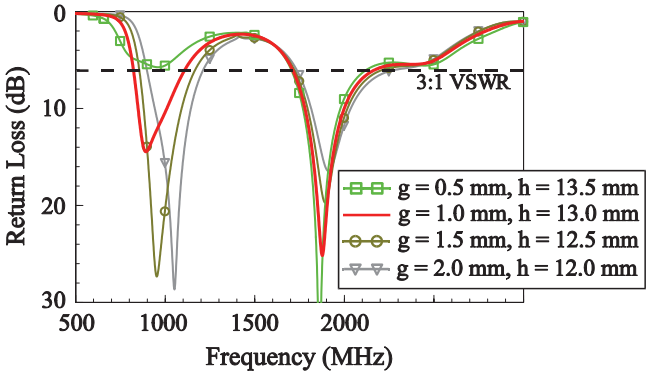

Figure 5 Simulated return loss as a function of the coupling-gap width g. Other dimensions are the same as studied in Figure 2. [Color figure can be viewed in the online issue, which is available at www.interscience.wiley.com]

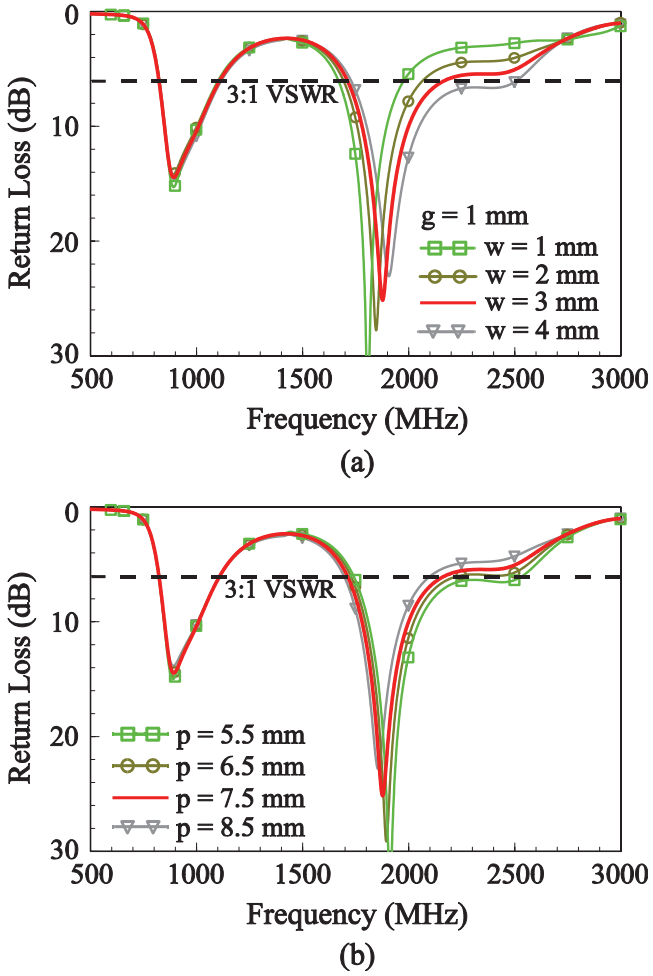

Figure 6 Simulated return loss as a function of (a) the coupling-section width w and (b) the end-section length p of the printed monopole. Other dimensions are the same as studied in Figure 2. [Color figure can be viewed in the online issue, which is available at www.interscience.wiley.com]

Figure 3 shows the comparison of the simulated return loss for the proposed antenna studied in Figure 2 and the case without the loop strip. It is clearly seen that, when the loop strip is not present, there is only one resonant mode controlled by the printed monopole excited. This agrees with the expectation described in Section 2. When the loop strip is present, the lower resonant mode with a wide bandwidth is generated.

Figure 4 shows the simulated excited surface currents at 900 and 1900 MHz on the antenna and the system ground plane. From the results shown in Figure 4(a), the excited surface currents indicate that the lower resonant mode is mainly controlled by the loop strip. This lower resonant mode can also be identified as the half-wavelength loop mode, because there is only one null current along the loop strip and it is located close to the central portion of the loop strip. On the other hand, the results at 1900 MHz [see Fig. 4(b)] show that the excited surface currents are much weaker on the loop strip than on the monopole strip. This indicates that the upper resonant mode is generated by the printed monopole operated as a quarter-wavelength structure.

Effects of the coupling-gap width g are studied in Figure 5, and the simulated results of the return loss for the width g varied from 0.5 to 2.0 mm are presented. Note that the length h of the front section of the printed monopole varies as the width g varies; other dimensions are the same as given in Figure 2. It is seen that the

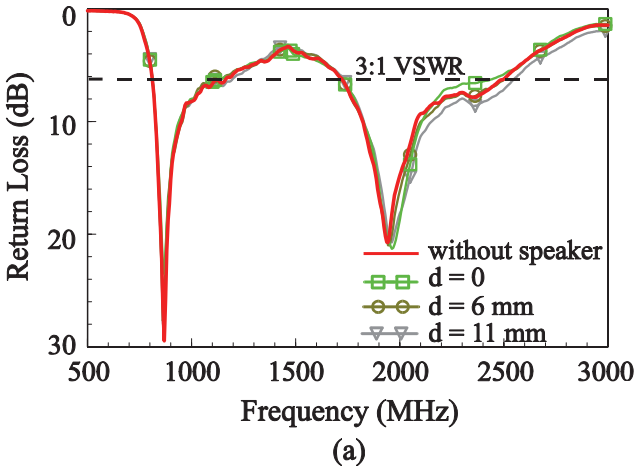

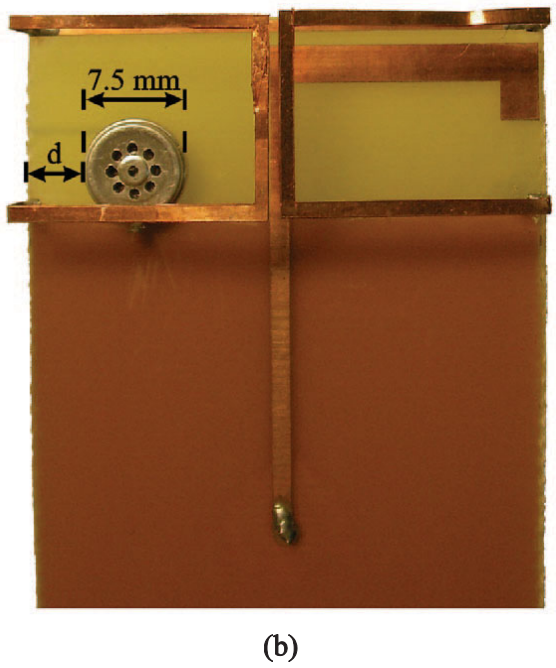

Figure 7 (a) Measured return loss for the antenna studied in Figure 2 with a practical speaker embedded inside the antenna region. (b) Experimental photo of the antenna with a practical speaker of diameter 7.5 mm. [Color figure can be viewed in the online issue, which is available at www.interscience.wiley.com]

upper resonant mode is very slightly affected by the width g. Conversely, large variations in the lower resonant mode are seen. When a smaller value of g is selected, the lower resonant mode is shifted to lower frequencies. However, the impedance matching of the lower resonant mode becomes poor when g is 0.5 mm only. Hence, in this study, the width g is selected to be 1 mm to shift the lower resonant mode to lower frequencies and also achieve good impedance matching over the excited resonant mode.

Effects of the dimensions of the printed monopole on the antenna performances are analyzed in Figure 6, in which the simulated return loss as a function of the coupling-section width w and the end-section length p are presented. In Figure 6(a), results for the width w varied from 1 to 4 mm are presented. There is almost no effect on the lower resonant modes of the antenna. On the other hand, the impedance matching for frequencies over the upper resonant mode is improved when the width w increases. By selecting the width w to be 3 mm, the obtained bandwidth is large enough for DCS/PCS/UMTS operation.

Effects of the end-section length p are shown in Figure 6(b). Again, there is almost no effect on the lower resonant mode of the antenna. Conversely, by varying the length p, the impedance matching over the upper resonant mode can be fine-adjusted. In this study, the length p is chosen to be 7.5 mm for covering the desired DCS/PCS/UMTS operation. From these results, it can be concluded that the lower resonant mode is mainly controlled by the loop strip only and is almost not affected by the dimensions of the printed monopole.

The case of embedding a practical speaker inside the antenna region is studied in Figure 7. The measured return loss as a function of d for the antenna studied in Figure 2 with a practical speaker is shown in Figure 7(a); d is the distance of the speaker from the edge of the circuit board [see Fig. 7(b), the experimental photo of the antenna embedded with a practical speaker of diameter 7.5 mm]. For the distance d varied from 0 (flushed to the edge of the circuit board) to 11 mm (very close to the front section of the printed monopole or the central line of the circuit board), the impedance matching over the lower resonant mode is generally not affected, whereas there are slight effects on the impedance matching over the high-frequency portion of the upper resonant mode. However, the obtained bandwidth still easily covers the desired DCS/PCS/UMTS operation.

Radiation characteristics of the antenna are also studied. Figures 8 and 9 plot the measured radiation patterns at 860, 925, 1795 1920, and 2045 MHz (center frequencies of GSM850, GSM900, DCS, PCS, and UMTS bands) for the antenna studied in Figure 2. In Figures 8(a) and 8(b), similar dipole-like radiation patterns at

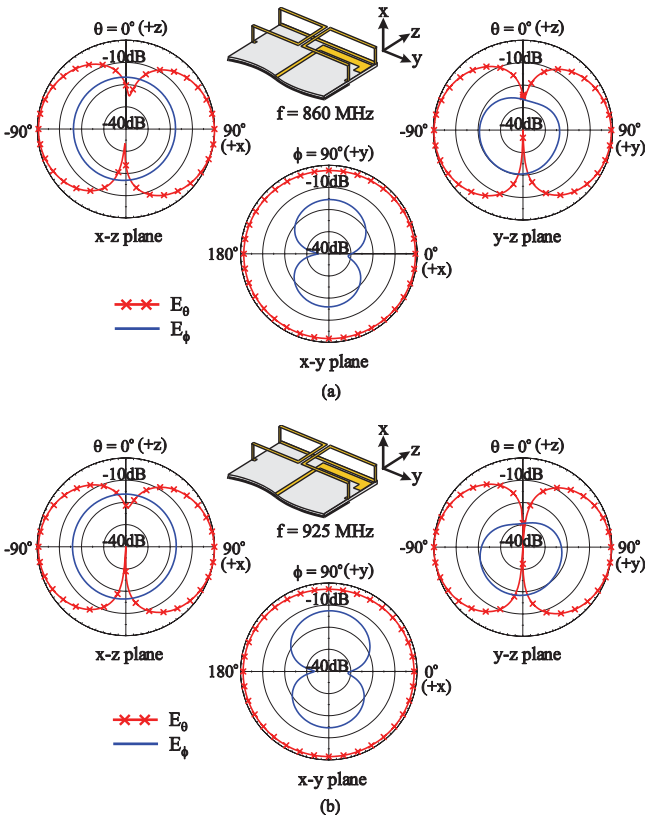

Figure 8 Measured radiation patterns at (a) 860 and (b) 925 MHz for the antenna studied in Figure 2. [Color figure can be viewed in the online issue, which is available at www.interscience.wiley.com]

860 and 925 MHz are seen, and omnidirectional radiation in the azimuthal plane (x–y plane) is observed. For the radiation patterns at 1795, 1920, and 2045 MHz shown in Figures 9(a)–9(c), more variations and nulls in the patterns are seen. These obtained patterns are in general similar to those observed for the conventional internal mobile phone antennas [6]. Figure 10 presents the measured antenna gain and simulated radiation efficiency for the antenna studied in Figure 2. For frequencies over the GSM850/900 band, the antenna gain is about −0.8 to 1.1 dBi and the radiation efficiency is over 60% [see Fig. 10(a)], whereas for the DCS/PCS/UMTS band it ranges from about 1.3 to 4.3 dBi and the radiation efficiency is all larger than 68% [see Fig. 10(b)].

4. CONCLUSION

A novel internal penta-band mobile phone antenna capable of integrating the nearby electronic element such as the speaker or the like in the mobile phone has been proposed. The antenna is formed by a half-wavelength loop strip mounted above the circuit board of the mobile phone and capacitively excited by a quarter-wavelength monopole printed on the circuit board. The antenna is configured to have a compact configuration ($6 \times 15 \times 40$ mm^3), yet it can accommodate the speaker with the antenna performances very slightly affected and generate two wide operating modes for covering GSM850/900/DCS/PCS/UMTS operation. Moreover, the lower and upper modes of the antenna can generally be controlled independently by the loop strip excited as a half-wavelength resonant mode and the printed monopole excited as a quarter-wavelength resonant mode. This feature makes it easy to fine-adjust the two excited resonant modes for the desired penta-band operation. Good radiation characteristics for frequencies over the five operating bands have also been obtained.

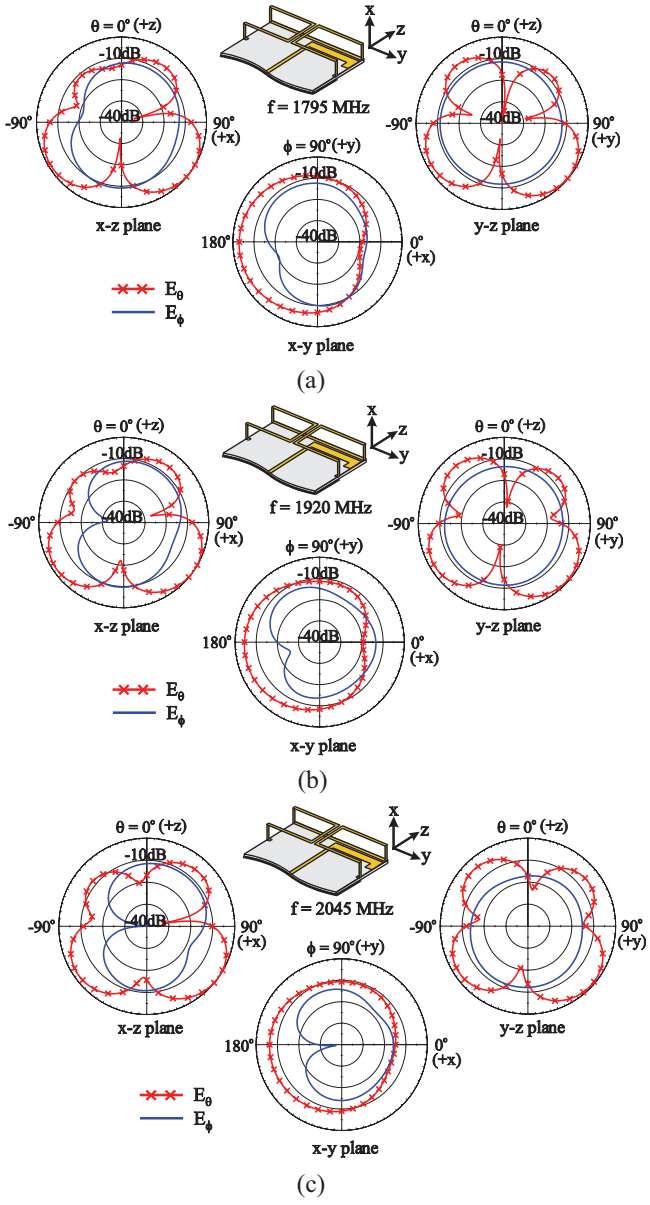

Figure 9 Measured radiation patterns at (a) 1795, (b) 1920, and (c) 2045 MHz for the antenna studied in Figure 2. [Color figure can be viewed in the online issue, which is available at www.interscience.wiley.com]

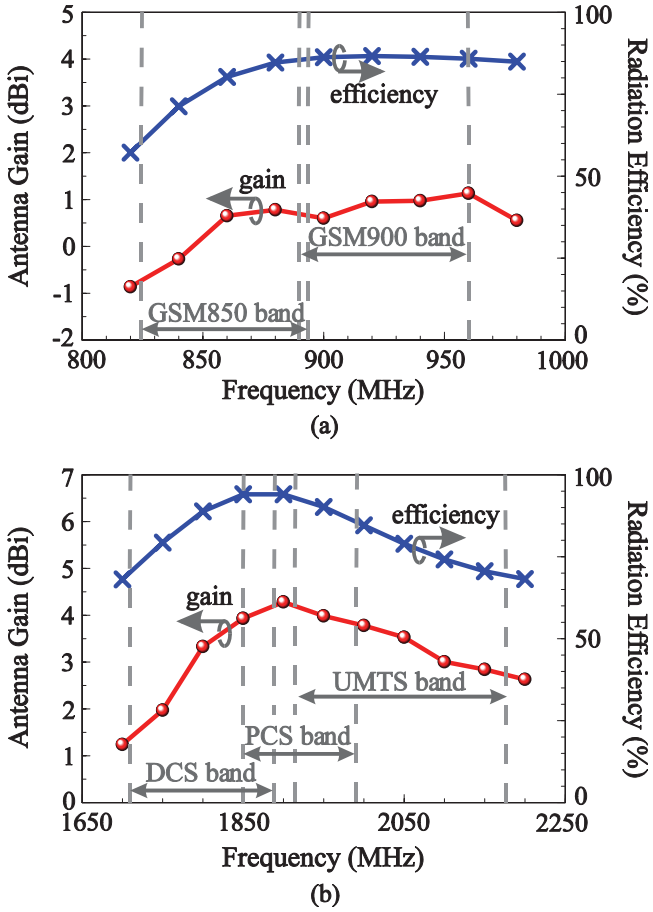

Figure 10 Measured antenna gain and simulated radiation efficiency for the proposed antenna studied in Figure 2. (a) The GSM850/900 band. (b) The DCS/PCS/UMTS band. [Color figure can be viewed in the online issue, which is available at www.interscience.wiley.com]

REFERENCES

1. B.K. Yu, B. Jung, H.J. Lee, F.J. Harackiewicz, and B. Lee, A folded and bent internal loop antenna for GSM/DCS/PCS operation of mobile handset applications, Microwave Opt Technol Lett 48 (2006), 463–467.
2. B. Jung, H. Rhyu, Y.J. Lee, F.J. Harackiewicz, M.J. Park, and B. Lee, Internal folded loop antenna with tuning notches for GSM/GPS/DCS/PCS mobile handset applications, Microwave Opt Technol Lett 48 (2006), 1501–1504.
3. C.I. Lin and K.L. Wong, Internal meandered loop antenna for GSM/DCS/PCS multiband operation in a mobile phone with the user's hand, Microwave Opt Technol Lett 49 (2007), 759–765.

4. Y.W. Chi and K.L. Wong, Internal compact dual-band printed loop antenna for mobile phone application, IEEE Trans Antennas Propag 55 (2007), 1457–1462.
5. W.Y. Li and K.L. Wong, Surface-mount loop antenna for AMPS/GSM/DCS/PCS operation in the PDA phone, Microwave Opt Technol Lett 49 (2007), 2250–2254.
6. K.L. Wong, Planar antennas for wireless communications, Wiley, New York, 2003.
7. C.H. Wu and K.L. Wong, Internal shorted planar monopole antenna embedded with a resonant spiral slot for penta-band mobile phone application, Microwave Opt Technol Lett 50 (2008), 529–536.
8. C.H. Chang, K.L. Wong, and J.S. Row, Multiband surface-mount chip antenna integrated with the speaker in the mobile phone, Microwave Opt Technol Lett 50 (2008), 1126–1132.
9. W.L. Stutzman and G.A. Thiele, Antenna theory and design, 2nd ed., Wiley, New York, 1998, pp. 172-173.
10. Y.L. Kuo and K.L. Wong, Printed double-T monopole antenna for 2.4/5.2 GHz dual-band WLAN operations, IEEE Trans Antennas Propag 51 (2003), 2187–2192.
11. K.L. Wong, Y.C. Lin, and B. Chen, Internal patch antenna with a thin air-layer substrate for GSM/DCS operation in a PDA phone, IEEE Trans Antennas Propag 55 (2007), 1165–1172.
12. W.Y. Li and K.L. Wong, Internal printed loop-type mobile phone antenna for penta-band operation, Microwave Opt Technol Lett 49 (2007), 2595–2599.
13. L.C. Chou and K.L. Wong, Uni-planar dual-band monopole antenna for 2.4/5 GHz WLAN operation in the laptop computer, IEEE Trans Antennas Propag 55 (2007), 3739–3741.
14. Ansoft Corporation HFSS. http://www.ansoft.com/products/hf/hfss/.

CMOS TOP-SERIES COUPLING QUADRATURE INJECTION-LOCKED FREQUENCY DIVIDER

Sheng-Lyang Jang, Sheng-Chien Wu, Chien-Feng Lee, and M.-H. Juang
Department of Electronic Engineering, National Taiwan University of Science and Technology, 43, Keelung Road, Section 4, Taipei, Taiwan 106, Republic of China; Corresponding author: D9202209@mail.ntust.edu.tw

Received 24 January 2008

ABSTRACT: *This article presents a new divide-by-2 injection-locked frequency divider (ILFD). The ILFD consists of a 2.1-GHz top-series quadrature voltage-controlled oscillator (QVCO) and two NMOS switches, which are in parallel with the QVCO resonators for signal injection. The proposed CMOS ILFD uses three-dimensional inductor to save chip area and has been implemented with the TSMC 0.18-μm CMOS technology and the core power consumption is 9.36 mW at the supply voltage of 0.9 V. The free-running frequency of the ILFD is tunable from 2.02 to 2.28 GHz. At the input power of −8 dBm, the total divide-by-2 locking range is from 3.6 to 6.05 GHz as the tuning voltage is varied from 0 to 0.9 V. The phase noise of the locked output spectrum is lower than that of free running ILFD in the ÷2 mode. The phase deviation of quadrature output is about 0.19°.* © 2008 Wiley Periodicals, Inc. Microwave Opt Technol Lett 50: 2554–2557, 2008; Published online in Wiley InterScience (www.interscience.wiley.com). DOI 10.1002/mop.23724

Key words: *CMOS; divide-by-2; injection locking frequency divider; quadrature voltage-controlled oscillator; 3D inductor*

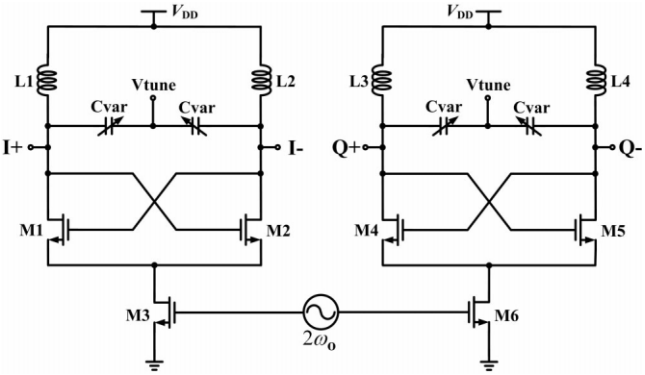

Figure 1 Schematic of a conventional divide-by-2 QILFD

1. INTRODUCTION

Frequency dividers (FDs) can take a sinusoidal input signal and generate a periodic output signal at a frequency that is a fraction of the input signal. LC tank FDs are widely used for low power and high frequency application. The cross-coupled LC-tank FDs are developed using a cross-coupled voltage-controlled oscillator (VCO) with tail injection [1] or direct injection [2]. These types of FDs can have even-order division and are frequently used in PLL and signal generators in a transceiver to down-convert radio frequency signal or up-convert base-band signal. The cross-coupled LC-tank FDs can be used as shown in Figure 1 to generate quadrature signals [1]. The phase accuracy of quadrature signals in Figure 1 depends on the phase accuracy of differential injection signals [3].

In this article, a new ÷2 LC tank FD, as shown in Figure 2, is proposed; it is based on a CMOS top-series quadrature VCO (QVCO) [4] with two injection MOSFETs in parallel with the resonator outputs. The proposed injection-locked FD (ILFD) provides quadrature outputs in the free-running mode, and it can be used as a ÷2 circuit with two differential injection ports. Section 2 describes the operation principle of the proposed ILFD circuit and the circuit constituent components. Section 3 describes the experimental results, and Section 4 is the conclusion.

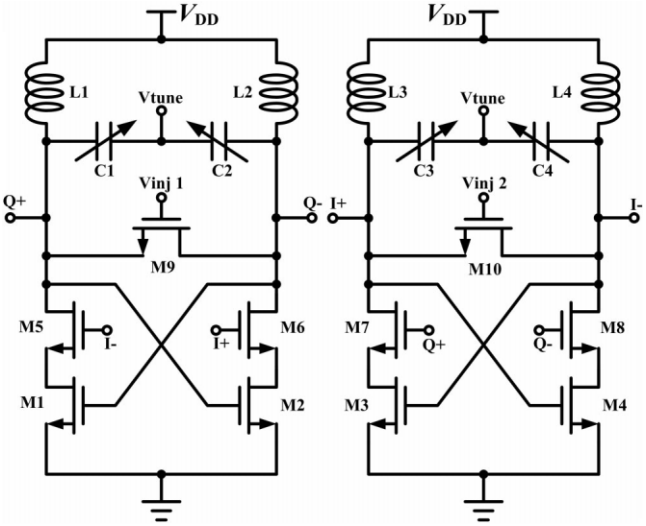

Figure 2 Schematic of the proposed QILFD. (a) 3D view of the used helical inductor; (b) simulated inductance and *Q*-factor of inductor versus frequency